The Journal of Immunology

This information is current as of June 5, 2015.

Scar-Associated Macrophages Are a Major Source of Hepatic Matrix Metalloproteinase-13 and Facilitate the Resolution of Murine Hepatic Fibrosis

Jonathan A. Fallowfield, Masashi Mizuno, Timothy J. Kendall, Christothea M. Constandinou, R. Christopher Benyon, Jeremy S. Duffield and John P. Iredale

J Immunol 2007; 178:5288-5295; ;
doi: 10.4049/jimmunol.178.8.5288
http://www.jimmunol.org/content/178/8/5288

References This article **cites 37 articles**, 11 of which you can access for free at:
http://www.jimmunol.org/content/178/8/5288.full#ref-list-1

Subscriptions Information about subscribing to *The Journal of Immunology* is online at:
http://jimmunol.org/subscriptions

Permissions Submit copyright permission requests at:
http://www.aai.org/ji/copyright.html

Email Alerts Receive free email-alerts when new articles cite this article. Sign up at:
http://jimmunol.org/cgi/alerts/etoc

The Journal of Immunology is published twice each month by
The American Association of Immunologists, Inc.,
9650 Rockville Pike, Bethesda, MD 20814-3994.
Copyright © 2007 by The American Association of Immunologists All rights reserved.
Print ISSN: 0022-1767 Online ISSN: 1550-6606.

Downloaded from http://www.jimmunol.org/ at North Dakota State Univ Lib/Periodicals Dept on June 5, 2015

Scar-Associated Macrophages Are a Major Source of Hepatic Matrix Metalloproteinase-13 and Facilitate the Resolution of Murine Hepatic Fibrosis[1]

Jonathan A. Fallowfield,* Masashi Mizuno,† Timothy J. Kendall,* Christothea M. Constandinou,‡ R. Christopher Benyon,* Jeremy S. Duffield,† and John P. Iredale[2§]

Both the identity and source of the rodent collagenase(s) that mediates matrix remodeling in liver fibrosis remain elusive. We have recently demonstrated an unequivocal role for scar-associated macrophages (SAMs) in the spontaneous resolution of liver fibrosis and sought to determine whether SAMs are the source of matrix metalloproteinase (MMP) 13 (collagenase 3), considered to be the primary interstitial collagenase in rodents. In this study, we demonstrate an association between MMP13 expression and the presence of SAMs in the regression of experimental liver fibrosis. *mmp13* gene expression was restricted to regions of fibrosis that were rich in SAMs. Both MMP13 mRNA and protein colocalized to large phagocytes within and directly apposed to hepatic scars. Using the *CD11b*-DTR-transgenic mouse to deplete SAMs in a model of chronic CCl_4 injury, we found that SAM depletion resulted in a 5-fold reduction in *mmp13* message ($p = 0.005$). Furthermore, resolution of CCl_4-induced fibrosis was retarded in MMP13-deficient mice. Thus, SAMs selectively, during resolution of fibrosis induce and use the major collagenase MMP13 to mediate the resorption of interstitial matrix and successfully remodel the fibrotic liver. *The Journal of Immunology,* 2007, 178: 5288–5295.

We have recently demonstrated an important role for macrophages in the normal resolution of hepatic fibrosis using a model of CCl_4-induced liver injury followed by spontaneous recovery in rodents (1). Using a conditional ablation mouse model to selectively deplete macrophages during the resolution phase of hepatic fibrosis, we observed failure to remodel interstitial collagen, particularly perisinusoidal fibrosis, as a result of the selective depletion of scar-associated macrophages (SAMs)[3] (1). We were therefore interested to discover the key effector molecules and mechanisms by which macrophages mediate this process.

Macrophages have been shown to produce gelatinases (matrix metalloproteinase (MMP)2, MMP9), metalloelastase (MMP12), matrilysin (MMP7), and collagenases (MMP1 and MMP13) in different circumstances (2, 3), allowing them to degrade complex extracellular matrices. Further support for an important role of the macrophage in matrix remodeling comes from in situ hybridization studies showing abundant MMP mRNA within macrophages in the rheumatoid synovial pannus (4), in atherosclerotic plaques (5), and in the lung during injury (6).

Remodeling of fibrillar collagen in rodents has been widely attributed to the action of MMP13, the main collagenase identified in this order. This consensus is based on unproductive attempts to detect the presence in rodent tissue of MMP1 (the major interstitial collagenase in humans) which suggests that MMP1 may be functionally substituted in rodents by MMP13 (7). Identifying the key collagenase(s) that mediates the regression of rodent liver fibrosis is pivotal to understanding models that are used in proof of concept studies of antifibrotic compounds in vivo (8–10).

MMP13 has potent proteinase activity against a wide variety of extracellular matrix components, particularly fibrillar collagens and gelatins. MMP13 has a central position in the MMP activation cascade, both activating and being activated by several MMPs (7, 11, 12). Active MMP13 is inhibited in a 1:1 stochiometric fashion by tissue inhibitors of metalloproteinases (TIMPs) 1, 2, and 3). Further regulation of MMP13 synthesis is mediated by cytokines (e.g., TGF-β), growth factors and probably also by interaction with the extracellular matrix via integrin-mediated pathways, thereby providing the matrix with a mechanism by which it can regulate its own composition.

In progressive liver disease in human and animal models of liver fibrosis, the level of expression of MMP1/MMP13 in most cases does not appear to alter significantly, whereas the expression of TIMP-1 and -2 is markedly increased (13, 14). In contrast, enhanced *mmp13* mRNA transcription during resolution of CCl_4-induced rat liver fibrosis has been reported (15). In this 8-wk model, *mmp13* expression was observed early and transiently between days 5 and 7 after cessation of injury.

The cellular origin of MMP13 remains controversial. Contrasting in vivo models have suggested that several cell types have the

*Liver Research Group, Southampton General Hospital, Southampton, United Kingdom; †Renal Division, Brigham and Women's Hospital and Harvard Medical School, Harvard Institutes of Medicine, Boston, MA 02115; ‡Cancer Research U.K. Institute for Cancer Studies, University of Birmingham, Birmingham, United Kingdom; and §Medical Research Council/University of Edinburgh Centre for Inflammation Research, Edinburgh, United Kingdom

Received for publication November 15, 2006. Accepted for publication January 22, 2007.

The costs of publication of this article were defrayed in part by the payment of page charges. This article must therefore be hereby marked *advertisement* in accordance with 18 U.S.C. Section 1734 solely to indicate this fact.

[1] This work was supported by grants from the Medical Research Council U.K. (to J.A.F., J.P.I., and R.C.B.); Wellcome Trust U.K. (to T.J.K.); National Institutes of Health Grant DK73299 (to J.S.D.); and also by generous donations from the estates of the late Victor Lyons and the late John Clarke.

[2] Address correspondence and reprint requests to Dr. John P. Iredale, Medical Research Council/University of Edinburgh Centre for Inflammation Research, Little France Way, Edinburgh, U.K. E-mail address: John.Iredale@ed.ac.uk

[3] Abbreviations used in this paper: SAM, scar-associated macrophage; MMP, matrix metalloproteinase; HSC, hepatic stellate cell; TIMP, tissue inhibitor of metalloproteinase; DT, diphtheria toxin; LCM, laser capture microdissection; WT, wild type; dig, digoxigenin; HPF, high power field.

Copyright © 2007 by The American Association of Immunologists, Inc. 0022-1767/07/$2.00

Downloaded from http://www.jimmunol.org/ at North Dakota State Univ Lib/Periodicals Dept on June 5, 2015

capacity to produce MMP13 in certain circumstances, including hepatic stellate cells (HSCs; Ref. 15), Kupffer cells (16), and stem cells (17) but with no clear consensus. Early liver injury, in particular, is characterized by a rich inflammatory infiltrate which includes recruited monocyte-macrophages. These may represent an alternative source of MMP13 or other enzymes with interstitial collagenase activity. Indeed, the initial surge in MMP13 expression in a model of acute liver toxicity appeared to parallel TNF-α expression and the presence of tissue inflammation (18).

We hypothesized that SAMs might represent the elusive cellular source of collagenolytic MMP13 in hepatic fibrosis. In this study, we show a temporal correlation between the level of MMP13 expression and the presence of macrophages in the injured and recovering liver after fibrotic injury and further localize MMP13 in vivo to SAMs. In addition, we have previously shown that conditional macrophage ablation inhibits remodeling of hepatic fibrosis (1), and in this study we demonstrate a similar fact when MMP13 is deleted. This supports a critical role for macrophage-derived MMP13 in mediating the regression of hepatic fibrosis.

Materials and Methods

Rodent carbon tetrachloride models

Animals were housed in standard sterile conditions with free access to chow and water. All manipulations and procedures were undertaken in accordance with United Kingdom Home Office license regulations and protocols approved by the Standing Committee on Animals of Harvard Medical School.

Progressive rat liver fibrosis demonstrating complete or incomplete spontaneous regression

Liver injury was induced as previously described (19). In brief, cohorts of 12 Sprague–Dawley rats were injected i.p. with 0.2 ml/100 g sterile CCl_4 dissolved in a 1:1 ratio with olive oil twice weekly for 4, 6, and 8 wk to generate an early reversible fibrosis and early and established cirrhosis, respectively. In addition, a cohort was treated for 12 wk to establish advanced micronodular cirrhosis which undergoes only partial resolution during 1 year of follow-up. For each model, animals were euthanized, and livers were harvested at peak fibrosis (immediately after the final injection of CCl_4) and at 3, 14, 28, 84, 168, and (in the 12-wk model) 366 days of spontaneous recovery ($n = 4$ at each time point in each model). Three normal, untreated rat livers were also harvested for use as controls in individual experiments. Harvested livers were split and fixed in formalin for subsequent immunohistochemical studies or snap frozen in liquid nitrogen for biochemical and molecular analysis.

Murine model of hepatic fibrosis and spontaneous resolution in CD11b-*DTR-transgenic mice*

Details of the generation of the *CD11b*-DTR mice have been described previously (1). In brief, adult *CD11b*-DTR mice (FVB/N) were injected with 0.25 μl/g CCl_4 i.p. twice weekly for 12 wk. During the 12th week, the mice were given by tail vein injection either: 1) diphtheria toxin (DT; 10 ng/g) immediately after the first injection of CCl_4 that week, DT 24 h later, and DT an additional 48 h later to coincide with the next injection of CCl_4; 2) DT (25 ng/g i.p.) over a similar schedule; or 3) 100 μl of PBS (i.v.) as control to coincide with the DT injections. Livers were harvested 24 h after the final dose of DT or PBS.

MMP13 knockout mouse model of hepatic fibrosis and spontaneous resolution

MMP13-deficient mice (*mmp13*$^{-/-}$) were a gift from Dr. S. Krane (Harvard Medical School, Boston, MA). The *mmp13*$^{-/-}$ mice were generated by gene targeting in embryonic stem cells as previously described (20). Genotype of the mice was verified by a two-step PCR using *Taq* polymerase (Qiagen) and the following primer pairs: primer 1/primer 3; primer 2/primer 3. Sequences were as follows: primer 1 (phosphoglycerate kinase) 5′-CGAAGGAGCAAAGCTGCTA-3′; primer 2 (exon 5F) 5′-TTTATTGT TGCTGCCCATGAG-3′; primer 3 (exon 6R) 5′-AGTTTCTCCTCG GAGACTGGT-3′. Conditions for PCR were 94°C for 3 min; then 40 cycles of 94°C for 45 s, 50°C for 45 s and 72°C for 2 min; then finally 72°C for 10 min.

Liver fibrosis was induced in cohorts of sex- and age-matched *mmp13*$^{-/-}$ and wild-type (WT) C57BL/6 mice by 4 wk, three-times-weekly i.p. administration of escalating doses of CCl_4 dissolved in sterile olive oil as follows: week 1, 0.125 ml/kg; week 2, 0.25 ml/kg; week 3, 0.5 ml/kg; week 4, 1 ml/kg. This escalating 4-wk CCl_4 protocol results in a rapid induction of advanced liver fibrosis (Q. Anstee, Imperial College, London, U.K., unpublished observations). Animals were euthanized at peak fibrosis (24 h after the final dose of CCl_4) and after 1, 3, and 5 days of spontaneous resolution ($n = 5$ at each time point). Four *mmp13*$^{-/-}$ and WT mice received olive oil only and served as vehicle controls. Harvested livers were split and fixed in formalin for subsequent immunohistochemical studies or snap frozen into liquid nitrogen for biochemical and molecular analysis.

Quantitation of mRNA level by real-time RT-PCR

RNA was purified from CCl_4-treated and olive oil-treated (control) livers using the RNAeasy method (Qiagen). First-strand cDNA synthesis was undertaken using random primers and murine Moloney leukemia virus reverse transcriptase (Promega). Primers and FAM-TAMRA probes were designed using the TaqMan Primer Express program, and real-time quantitation was obtained using the PE Applied Biosystems 7700 Sequence Detection System. The following were primers/probes for rat: *mmp13*, sense 5′-GGTTGAGCCTGAACTGTTTTTGA-3′, antisense 5′-CTCGTA TGCAGCATCCACATG-3′ and probe 5′-AGTCCTTTTGGCCAGAACT TCCC-3′ (Oswel Research Products); GAPDH, sense 5′-GGCCTACATG GCCTCCAA-3′, antisense 5′-TCTCTCTTGCTCTCAGTATCCTTGC-3′, and probe 5′-AGAAACCCTGGACCACCCAGCCC-3′ (Oswel Research Products). The following were primers/probes for mouse: *mmp2*, sense 5′-CCCCATGAAGCCTTGTTTACC-3′, antisense 5′-TTGTAGGAGGTG CCCTGGAA-3′, and probe 5′-GAATGCTGATGGACAGCCCTGCA0-3′ (Sigma-Genosys). Primers and probes for mouse MMP8 and MMP14 were custom designed and supplied by Primer Design. 18S rRNA Control Reagents (VIC probe) were manufactured by Applied Biosystems.

First-strand cDNA (1 μl = 10 ng of RNA), 0.3 μM concentrations of primers and 0.3 μM concentrations of probe were used in a 25-μl real-time TaqMan reaction using 2× Universal Master Mix (Applied Biosystems). Conditions were as follows: 50°C for 2 min; then 40 cycles of 95°C for 10 min, 95°C for 15 s, and 60°C for 1 min. All reactions were performed in triplicate. After detection of the threshold cycle for each mRNA in each sample, relative concentrations were calculated and normalized to control genes GAPDH or 18S. Products were run on an agarose gel to confirm a single band of the correct size.

In situ hybridization

mmp13 and *timp1* transcripts were detected in situ using oligonucleotide probes purchased from GeneDetect. All other reagents were supplied by DakoCytomation for oligoprobes and Roche for riboprobes unless stated otherwise.

mmp13 mouse antisense GreenStar digoxigenin (dig)-labeled oligoprobe hybridizes to nt 158–205 located within the coding sequence of NM_008607. Two antisense riboprobes and their sense counterparts were also synthesized by cloning nucleotide sequences from positions 24–440 and 805–1240 into the pCR^{R}2.1 linearized plasmid vector. After sequencing, dig-labeled probes were generated using the T7 promoter system (Promega). Both the size and extent of dig-labeling of probes were confirmed.

timp1 mouse antisense GreenStar dig-labeled oligoprobe hybridizes to nt 294–341 located within the coding sequence of NM_011593.

Tissue sections of 7 μm were cut under RNase-free conditions, dewaxed in xylene, and rehydrated through graded alcohols, then permeabilized with proteinase K at room temperature for 5 min. The protease was quenched in glycine (0.2% w/v in 1× PBS); then sections were rinsed in PBS and postfixed in paraformaldehyde (4% w/v in PBS), and endogenous peroxidase was blocked with hydrogen peroxide (1% w/v in methanol). Sections were prehybridized with mRNA in situ hybridization solution for 2 h at 37°C. Probes (sense control and antisense) were added at 200 ng/ml in hybridization solution overnight at 37°C. After stringency washes (1× SSC, 0.5× SSC, 0.1× SSC twice each for 15 min) and blocking with culture medium (DMEM, 20% FCS, 0.5% BSA), sections were incubated with rabbit anti-dig-HRP Ab (1/100) in buffer (100 mM Tris-HCl, 150 mM NaCl (pH 7.5) with 1% rabbit serum) or with anti-dig alkaline phosphatase for riboprobes, overnight at 4°C. For oligoprobes, avidin-biotin block (Vector Laboratories) was followed by signal amplification using the Genpoint tyramide kit, and color was developed with diaminobenzidine (Vector Laboratories). For riboprobes, lamivudine block was performed, and 5-bromo-4-chloro-3′-indolyphosphate *p*-toluidine salt was used as the color substrate. Sections were briefly counterstained in Meyer's hematoxylin (Gurr) or nuclear Fast Red (Sigma-Aldrich) for riboprobes and then

Downloaded from http://www.jimmunol.org/ at North Dakota State Univ Lib/Periodicals Dept on June 5, 2015

mounted in aqueous medium and dried in an incubator before microscopic analysis.

Laser capture microdissection (LCM)

The Leica laser microdissection microscope (ASLMD) was used to excise cell groups of histological tissue sections. Conventional microscopy slides were coated with a synthetic membrane held in place by a gene frame. Membrane-coated slides were then UV irradiated to destroy RNases. Snap frozen liver samples were mounted in OCT, and 10-μm sections were cut using a cryostat onto the membrane side of the slides. Tissue sections were fixed briefly in 70% ethanol, before nuclear counterstaining with Meyer's hematoxylin (Gurr). For dehydration, the sections were immersed for 30 s each in 70% ethanol, 95% ethanol, and for 60 s in absolute ethanol. Processed slides were stored in a desiccator containing silica gel for at least 3 days before LCM. Tissue of interest was cut and captured directly into 50 μl of guanidine thiocyanate-containing lysis buffer plus 2-ME (0.7 μl/100 μl of lysis buffer). Visualization and cutting were conducted at $\times$200 magnification. Previous work determined that at least 1×10^6 μm^2 of excised tissue was required for reliable RNA extraction and cDNA synthesis.

The Absolutely RNA Microprep kit (Stratagene) was used for RNA extraction according to manufacturer's instructions. First-strand cDNA was synthesized from 7.7-μl RNA samples using random hexamers and Impromptu Reverse Transcriptase (Promega). cDNA was used for real-time RT-PCR as described above. We controlled for the area of tissue dissected (1×10^6 μm^2) and used RT-PCR for β-actin to assess integrity of extracted RNA before real-time mRNA quantitation with normalization to 18S rRNA.

Immunohistochemistry

Rat SAMs were detected in 4-μm paraffin sections using ED-1 Ab (1/150; Serotec) after citrate/microwave Ag retrieval as previously described (1). MMP13 was detected in rat liver by incubation with mouse monoclonal anti-MMP13 (1/80 dilution, clone VIII A2; Biocarta) after citrate/microwave Ag retrieval. After blocking endogenous peroxidase (hydrogen peroxide, 0.3% w/v in methanol), endogenous avidin-biotin and incubating with culture medium (DMEM, 20% FCS, 0.5% BSA), the Universal Quick Kit (Vector Laboratories) was used for Ag detection. Diaminobenzidine or Fast Red (Vector Laboratories) were used as chromogens, and counterstaining was with Meyer's hematoxylin (Gurr).

H&E or picrosirius red were used for histochemical analysis of paraffin sections as previously described (19).

Assessment of tissue sections

Rat SAMs in H&E-stained sections were counted in 10 randomly selected high power fields (HPF) by two independent, blinded observers. A positive cell was identified on the basis of characteristic morphology, a nucleus and brown intracellular pigment (ceroid) as evidence of phagocytosis (21) and included only if it was within or apposed to the scar. Counts were expressed as mean score $\pm$ SD.

For morphometric analysis of picrosirius red-stained collagen, 10 serial images from $n = 3$ control (olive oil) and $n = 5$–6 CCl_4-treated *mmp13*$^{-/-}$ and WT mice were digitally captured in a blinded manner at $\times$200 magnification. The area of collagen staining was measured using Fovea Pro (Reindeer Graphics) (1), and results are expressed as mean $\pm$ SE and groups compared using an unpaired Student *t* test. $p < 0.05$ was considered statistically significant.

Results

mmp13 *transcript level during spontaneous resolution of rat* CCl_4 *liver fibrosis parallels the relative abundance of SAMs*

Rats, treated for 4, 6, 8, and 12 wk with CCl_4, developed liver fibrosis with increasing histopathological severity and diminishing degrees of reversibility. Indeed, remodeling of scar after 4 wk of injury led to a rapid restitution of normal or near-normal liver architecture, but 12 wk of injury induced an advanced micronodular cirrhosis from which incomplete resolution occurred (13, 19). To evaluate the potential role of MMP13 in the regression of liver fibrosis, we studied the expression profile of *mmp13* mRNA using real-time RT-PCR during spontaneous resolution of the 12-wk CCl_4 rat cirrhosis model (Fig. 1*A*). *mmp13* transcript was up-regulated after cessation of CCl_4 injury, increasing 70-fold relative to untreated control liver at day 14 of resolution. Thereafter, mRNA expression declined significantly with time. This pattern

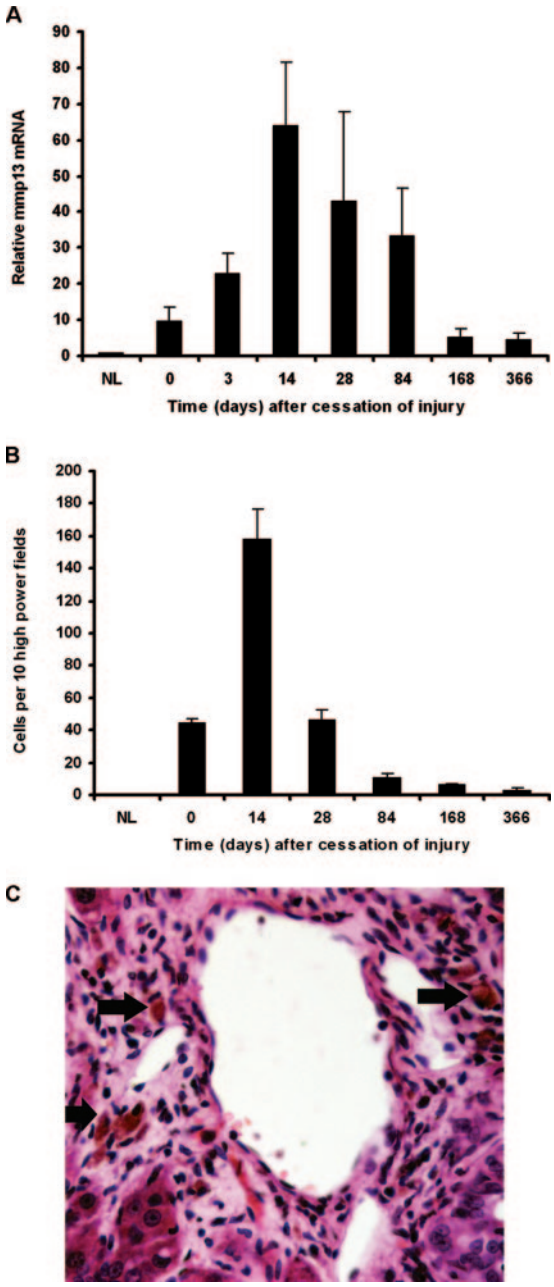

FIGURE 1. *mmp13* transcript is up-regulated during resolution of liver fibrosis in rats and correlates with the relative abundance of SAMs. *A*, *mmp13* mRNA expression (relative to 18S RNA and normal liver) during spontaneous resolution of advanced liver fibrosis after 12-wk CCl_4 injury ($n = 4$ per time point). Transcript was detected at low levels in normal untreated liver. There was a 10-fold increase in transcript level at peak fibrosis. However, this increased 70-fold at day 14 of resolution. *mmp13* transcript levels remained markedly elevated for a protracted period during the resolution of fibrosis in this rat model of remodeling. *B*, SAM numbers during resolution in 12-wk CCl_4 rat liver fibrosis. SAM numbers (defined as ceroid-containing cells with macrophage morphology within or apposed to scar) were increased 40-fold compared with normal livers (NL). However, during the early resolution phase, the number increased further and remained markedly elevated 28 days after injury. Even 366 days after cessation of CCl_4 injury, a small number of these cells remained apposed to the residual fibrotic bands. Note the correlation between SAM numbers and whole liver *mmp13* mRNA during spontaneous resolution. *C*, Macrophages were identified in H&E-stained sections as described above, and examples are shown (arrows) associated with an area of hepatic scarring at day 14 during the recovery phase.

Downloaded from http://www.jimmunol.org/ at North Dakota State Univ Lib/Periodicals Dept on June 5, 2015

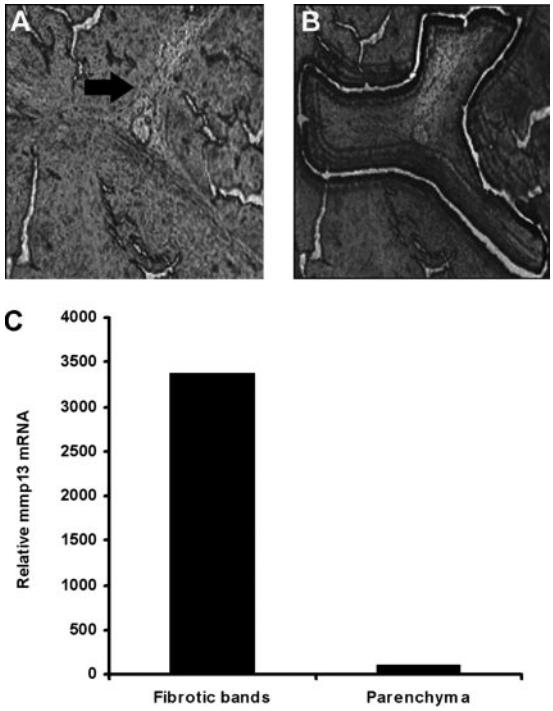

FIGURE 2. Relative *mmp13* transcript level in fibrotic bands and parenchyma. *A* and *B*, Fibrotic bands were separated from nonscarred liver parenchyma in tissue sections by LCM in CCl_4-treated rat liver at day 14 of recovery. *C*, *mmp13* transcript level (relative to 18S rRNA) was 34-fold higher in the dissected fibrotic bands relative to parenchymal tissue in the recovering rat liver.

of expression was consistent with our previous histological data, which showed that the majority of matrix remodeling had occurred by day 84 after cessation of injury (19).

There was a close relationship between the relative expression of *mmp13* mRNA and the number of SAMs during resolution of injury in the rat model (Fig. 1, *A* and *B*), suggesting that SAMs might be a major source of MMP13.

Persistent experimental liver fibrosis is associated with reduced numbers of SAMs

We investigated the population dynamics of SAMs in our 12-wk model of advanced micronodular cirrhosis by direct counting of scar-related ceroid-laden cells with typical macrophage morphology, thus defining a highly phagocytic population of macrophages (Fig. 1, *B* and *C*). Although macrophages were numerous early in resolution, being most abundant at 14 days after cessation of injury, late recovery was characterized by a paucity of macrophages and incomplete remodeling of fibrotic scars even after 366 days of spontaneous resolution. These findings suggest that the presence of SAMs may be a requirement for complete histological resolution of advanced fibrosis. Indeed, in the 4-wk rat CCl_4 injury model where complete remodeling of fibrosis occurs, SAMs persist throughout the brief recovery period with an average of 13 cells per HPF remaining after 28 days of spontaneous regression (1, 13).

During spontaneous resolution, mmp13 *transcript is confined exclusively to regions of hepatic fibrosis, rich in SAMs*

Quantitation of whole liver mRNA gives little information regarding topographical variations in gene expression. To study the hepatic scars and adjacent milieu, we used LCM to select areas of hepatic scarring and areas of unscarred parenchyma (Fig. 2, *A* and *B*). This technique allowed location specific quantitation of gene expression. Using real-time RT-PCR, we observed that *mmp13* mRNA was restricted to areas of resolving fibrosis, rich in SAMs (Fig. 2*C*).

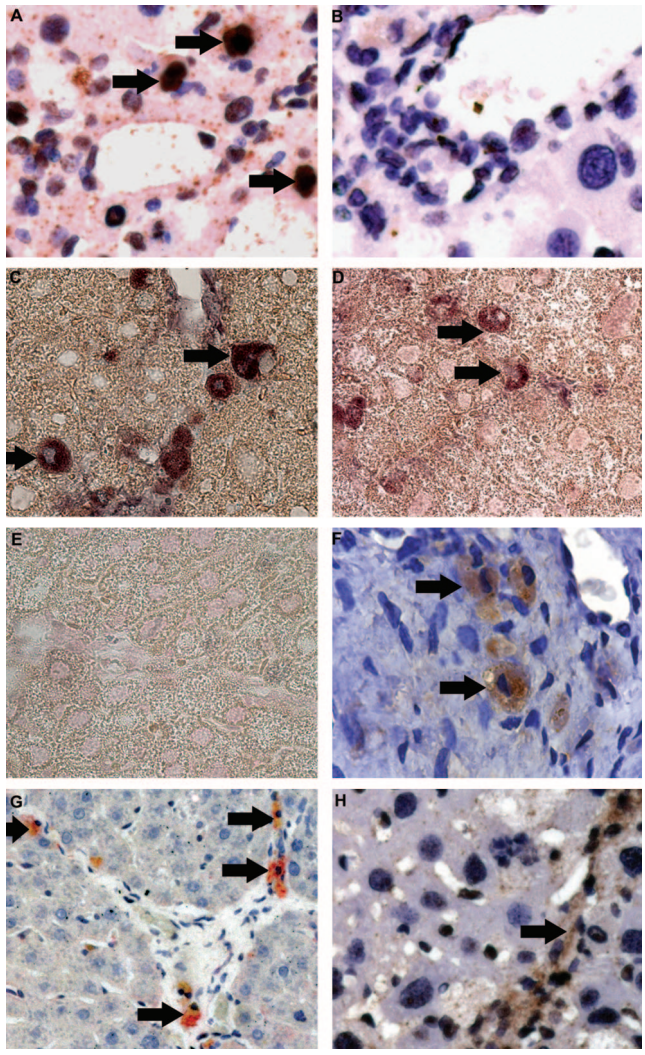

FIGURE 3. SAMs are the primary cellular source of MMP13 in resolving liver fibrosis in rodents. *A–E*, Representative sections showing *mmp13* transcript localization by in situ hybridization in mouse CCl_4 fibrosis recovery model. Using an oligonucleotide probe (*A*, antisense; *B*, sense control), *mmp13* antisense identified a population of large scar-associated phagocytes. The same cells were detected during resolution using two separate riboprobes (*C* and *D*) and sense control (*E*) was again negative. *F*, MMP13 protein was detected by immunohistochemistry in cells that resembled macrophages morphologically. *G*, Dual immunostaining for MMP13 protein (brown) and pan-macrophage marker ED-1 (red) confirmed colocalization of the protease to SAMs in rats. *H*, *timp1* transcript by in situ hybridization in mouse CCl_4 fibrosis recovery model. At peak fibrosis, *timp1* transcript was localized to scar within spindle-shaped cells. All original magnifications, ×400.

mmp13 *transcript localizes to scar-associated phagocytes in resolving mouse liver fibrosis*

The hepatic scar and its interface constitute a heterogeneous cell population. To establish the cellular source of *mmp13*, we used in situ hybridization in a murine CCl_4 model of liver fibrosis. We used a short oligonucleotide probe and, in addition, two ~400-bp RNA riboprobes to reinforce the specificity of our findings. By both methods, we identified a population of large rounded scar-associated phagocytes as the principal source of

Downloaded from http://www.jimmunol.org/ at North Dakota State Univ Lib/Periodicals Dept on June 5, 2015

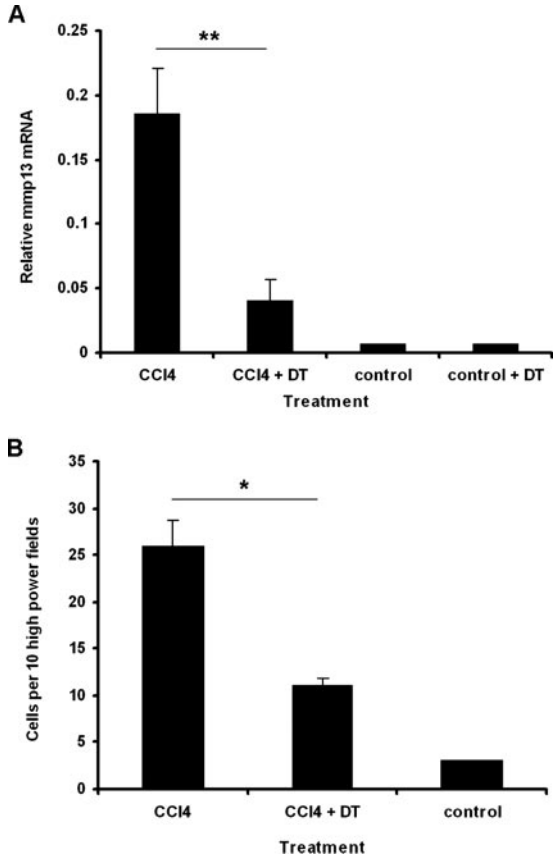

FIGURE 4. Conditional macrophage depletion curtailed *mmp13* mRNA transcript production to a level consistent with the proportion of macrophages depleted after 12-wk CCl_4 injury in *CD11b*-DTR-transgenic mice. *A*, Whole liver extracts were subjected to real-time RT-PCR for *mmp13* transcript. Macrophage depletion after administration of DT resulted in a 5-fold reduction in *mmp13* transcript level ($p = 0.005$; mean ± SE). *mmp13* mRNA was normalized to GAPDH ($n = 4$ animals per treatment). *B*, The number of cells expressing *mmp13* mRNA were also reduced by in situ hybridization ($p = 0.014$; mean ± SE).

mmp13 (Fig. 3, *A–E*), but there was no evidence that HSCs or myofibroblasts contained *mmp13* transcripts. Moreover, SAMs were well placed to facilitate matrix degradation, lying within and apposed to fibrotic scars. HSCs did, however, express abundant *timp1* (Fig. 3*H*), high levels of which suppress local MMP activity during progressive fibrosis and inhibit apoptosis of activated myofibroblasts (13). Note the morphological distinction between the SAMs producing *mmp13* transcript (Fig. 3, *A*, *C*, and *D*) and the HSCs producing *timp1* (Fig. 3*H*).

MMP13 protein colocalizes to SAMs

Having detected *mmp13* mRNA in cells that resembled macrophages morphologically, we immunolocalized the cellular protein. MMP13 protein was detected in cells with histological features of SAMs (Fig. 3*F*) and having similar topography to the population of phagocytes observed using in situ hybridization. Dual immunostaining using the cytoplasmic pan-macrophage marker ED-1 (the rat equivalent of human CD68) confirmed that MMP13-positive cells were SAMs (Fig. 3*G*) in rat liver tissue. There are no anti-mouse MMP13 Abs that identify the protein in tissue sections. Eighty-three percent of ED-1-positive SAMs costained for MMP13 at day 14 of resolution in the 12-wk rat CCl_4 model. Importantly, immunohistochemistry

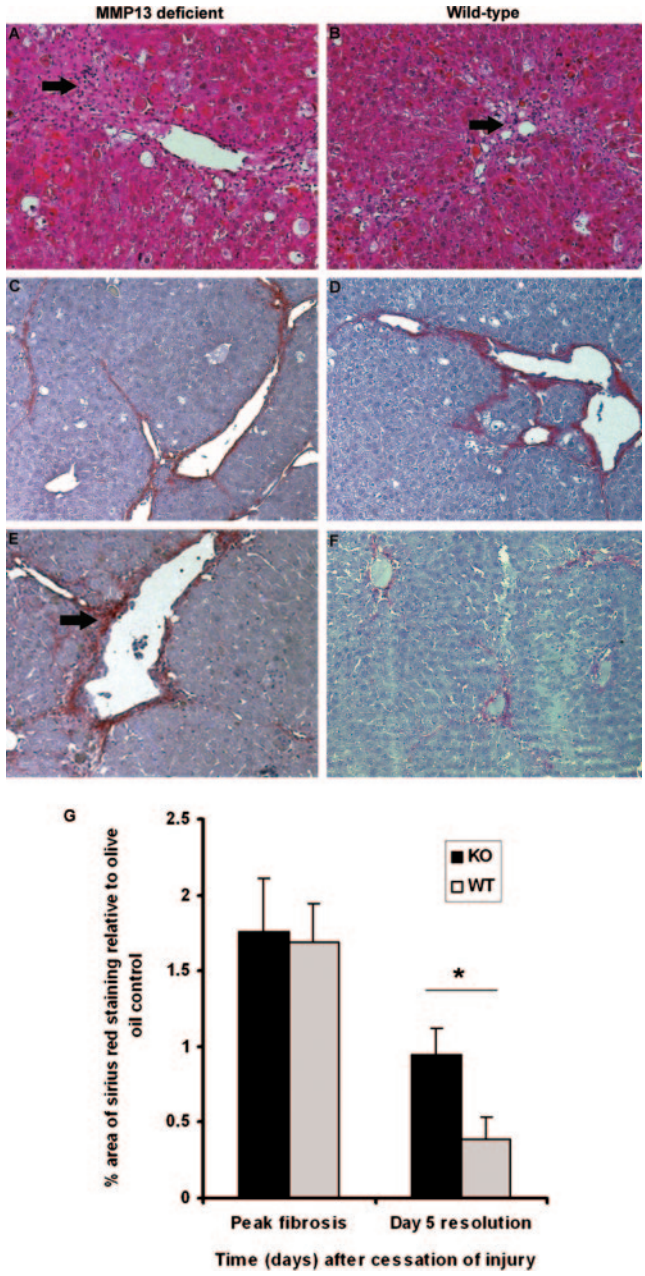

FIGURE 5. Remodeling of septal and perisinusoidal fibrosis is retarded in mice deficient in MMP13. *A* and *B*, CCl_4-induced hepatic injury in $mmp13^{-/-}$ and WT mice. Analysis of H&E-stained sections at peak fibrosis revealed comparable necroinflammatory injury in $mmp13^{-/-}$ (*A*) and WT (*B*) animals. Typical changes associated with CCl_4 damage were seen comprising fatty metamorphosis, zone III (centrilobular) necrosis, and a prominent inflammatory infiltrate (arrow) which included neutrophils and macrophages. *C–G*, Collagen staining by picrosirius red at peak fibrosis demonstrated significant pericentral collagen deposition with bridging fibrotic bands in both $mmp13^{-/-}$ (*C*) and WT (*D*) mice. *E* and *F*, After 5 days of spontaneous resolution, considerable matrix remodeling had occurred in the WT livers (*F*), but this process was attenuated in $mmp13^{-/-}$ mice (*E*) with persistence of septal collagen bands and perisinusoidal fibrosis (arrow). *G*, Morphometric quantitation of picrosirius red staining revealed a similar degree of collagen deposition in $mmp13^{-/-}$ and WT mice at peak injury, but by day 5 there was a clear difference with attenuated collagen degradation in the livers of $mmp13^{-/-}$ mice compared with WT counterparts ($p < 0.05$). Original magnifications, ×100. KO, Knockout.

revealed that apart from occasional spindle-shaped cells, there were no other discernable cell types within the liver with consistent MMP13 positivity.

Downloaded from http://www.jimmunol.org/ at North Dakota State Univ Lib/Periodicals Dept on June 5, 2015

Table I. *Expression of other MMPs with potential interstitial collagenase activity in MMP13 gene knockout mice*[a]

	Control	Peak Fibrosis	Day 1 Recovery	Day 3 Recovery	Day 5 Recovery
MMP2					
KO	1	8.47 ± 3.06	8.19 ± 3.8	20.06 ± 9.7	16.49 ± 11.5
WT	1	3.18 ± 0.62	4.72 ± 2.74	16.3 ± 14.2	5.68 ± 4.9
		NS	NS	NS	NS
MMP14					
KO	1	3.43 ± 0.74	14.2 ± 4.6	7.2 ± 3.5	11.1 ± 5.7
WT	1	4.12 ± 1.11	6.49 ± 2.98	2.49 ± 0.12	8.6 ± 7.8
		NS	NS	NS	NS
MMP8					
KO	1	5.26 ± 3.53	2.34 ± 1.3	0.39 ± 0.28	1.81 ± 1.37
WT	1	1.57 ± 1.01	3.66 ± 1.35	0.41 ± 0.19	0.23 ± 0.1
		NS	NS	NS	NS

[a] MMP mRNA was normalized to ribosomal 18S and expressed relative to control olive oil-treated liver. Values represent fold increase in mRNA expression ± SE. n = 3–5 animals per time point. KO, Knockout.

Conditional macrophage depletion results in attenuation of mouse mmp13 *transcript levels*

We used a conditional macrophage ablation mouse model (*CD11b*-DTR) to study the effect of depletion of SAMs on hepatic *mmp13* transcript level after CCl_4 injury (1). This model uses the low affinity of mouse DT receptor (heparin-binding epidermal growth factor receptor) compared with the human receptor. Transgenic expression of the human DT receptor confers sensitivity in mice only in macrophages and permits ablation in vivo after toxin injection. The *CD11b*-DTR construct uses the *CD11b* gene-regulatory elements for macrophage-specific expression. Using this model, monocytes in the circulation are depleted by 77 ± 14% (22) following DT, and macrophages in the liver scars are depleted by 78 ± 9% (1). In transgenic mice depleted of SAMs, we observed a 5-fold reduction in *mmp13* transcript level ($p = 0.005$) by real-time RT-PCR of whole liver extracts (Fig. 4*A*). The number of *mmp13*-positive cells was also decreased ($p < 0.05$) by in situ hybridization (Fig. 4*B*).

MMP13 gene knockout retards spontaneous resolution of experimental liver fibrosis

We induced advanced liver fibrosis with 4-wk CCl_4 injury in cohorts of MMP13-deficient and WT mice and allowed them to recover spontaneously for up to 5 days. Livers were harvested at peak fibrosis (24 h after final injection of CCl_4) and at day 1, day 3, and day 5 after cessation of injury. Analysis of H&E-stained sections at peak fibrosis revealed equivalent necroinflammatory injury in *mmp13*$^{-/-}$ and WT mice (Fig. 5, *A* and *B*). Immunohistochemistry for infiltrating neutrophils and macrophages showed no differences in hepatic inflammatory cell recruitment. At peak fibrosis, the mean number of neutrophils counted per HPF in the livers of *mmp13*$^{-/-}$ mice (65 ± 8.6) was similar to that of WT mice (57.6 ± 3.3). Furthermore, $CD68^+$ SAM numbers per 10 HPF in *mmp13*$^{-/-}$ mice (3.56 ± 0.48) were not statistically different to WT mice (3.12 + 0.22) at peak fibrosis and throughout the recovery period (data not shown).

After picrosirius red staining for collagen, extensive and comparable scarring was observed at peak fibrosis in both *mmp13*$^{-/-}$ and WT livers but not in vehicle (olive oil) controls (Fig. 5, *C* and *D*). However, remodeling of fibrosis was retarded in MMP13-deficient mice throughout the period of resolution. Quantitation of the picrosirius red area of staining by morphometry at day 5 of recovery ($p < 0.05$) confirmed the retarded remodeling phenotype (Fig. 5*G*), where residual septal bands and perisinusoidal fibrosis persisted in *mmp13*$^{-/-}$ livers in contrast to the WT livers where only minimal scarring remained (Fig. 5, *E* and *F*).

MMP13 deficiency did not abrogate regression of fibrosis completely, only retarded regression. One possible explanation is that other MMPs might take on additional roles in this mouse model. Real-time RT-PCR was used to determine whether *mmp13* gene disruption had resulted in compensatory alterations in the expression of other candidate collagenases (Table I). Although there were trends toward increased mRNA expression of *mmp2*, *mmp8*, and *mmp14* in *mmp13*$^{-/-}$ mice relative to WT animals, the differences were not statistically significant.

Discussion

For the first time, we have shown clear evidence that SAMs are a major source of MMP13 in resolving liver fibrosis. The observed phenotype in MMP13-deficient mice suggests that this collagenase plays a role in macrophage-directed remodeling of scar. Macrophages have been shown to promote resolution of liver fibrosis (1) and regulate repair processes in other organs (23–27). We hypothesized that SAMs were a potential source of hepatic MMP13 during regression of advanced fibrosis. To determine its expression profile, cellular source, and relative importance in vivo in mediating scar remodeling, we have used a series of distinct but complementary animal models.

Previous experiments using CCl_4 models of rat liver fibrosis demonstrate that SAMs populate hepatic scars during injury and repair (1). The number of SAMs increased in proportion to the duration of CCl_4 treatment, but they were also associated with resolving scar during spontaneous resolution. In the current study, hepatic MMP13 protein expression also increased as the period of CCl_4 injury was extended from 4 through 12 wk (our unpublished observation). This temporal correlation between SAM accumulation and MMP13 production was even more pronounced during regression of fibrosis. After 12 wk of CCl_4, we observed a prolonged increase in hepatic *mmp13* transcript above peak fibrosis levels extending to 84 days of recovery, suggesting that MMP13 was actively engaged in the remodeling process. Marked up-regulation was seen as early as 3 days after cessation of injury, with maximal mRNA expression being at day 14 of resolution (Fig. 1*A*). Furthermore, once SAMs had been lost from the recovering liver, further degradation of the fibrotic bands was minimal. These results differ from our earlier findings in the 4-wk fully reversible rat CCl_4 model, where *mmp13* transcript level was increased at peak fibrosis and remained elevated during 28 days of resolution

Downloaded from http://www.jimmunol.org/ at North Dakota State Univ Lib/Periodicals Dept on June 5, 2015

(13). SAMs were apparent throughout the remodeling phase, suggesting that their presence (and production of MMP13) might be a critical determinant of complete histological restitution.

Macrophages are recognized to be a major source of MMPs (2, 3) and can influence matrix turnover both directly by producing MMPs (24) and indirectly by secretion of cytokines including IL-1 and TNF-α that modulate MMP production by other resident cell types (25). We have provided compelling evidence, by both in situ hybridization (Fig. 3, *A–E*) and immunohistochemical staining (Fig. 3*F*), that macrophages represent the primary source of MMP13 in relevant models of hepatic fibrosis; findings that were later confirmed using macrophage-specific markers (Fig. 3*G*). These macrophages were seen almost exclusively within areas of scarring (SAMs) and therefore were ideally situated to facilitate matrix degradation. Moreover, when areas of fibrosis and unscarred liver tissue were separately dissected out by LCM, we detected *mmp13* mRNA only in and around the scars.

The *CD11b*-DTR-transgenic mouse model provided a robust system to selectively deplete the cell population of interest (SAM) and observe any downstream effect on *mmp13* transcript level and resolution of fibrosis. Our data show that macrophage depletion resulted in a 5-fold reduction in *mmp13* transcript level by real-time RT-PCR, results that were consistent with subsequent experiments using in situ hybridization and counting of *mmp13*-positive cells, supporting the hypothesis that SAMs represent a major (but not exclusive) cellular source. DT administration did not abolish hepatic MMP13 entirely, a possible explanation being that macrophage depletion is not absolute in this model (1).

It is plausible that other cells capable of expressing MMPs may also contribute to matrix degradation by releasing collagenolytic enzymes into the pericellular milieu. Previous studies have documented transient expression of MMP13 by HSCs activated by primary culture on plastic (13) or after TNF-α (18) or halofuginone (28) administration, but the relevance of these observations to HSCs in vivo remains uncertain. More recently, Watanabe et al. (15) also suggested that HSCs are a source of MMP13. However, earlier work using 4- and 8-wk CCl_4 resolution models, together with the data in this study, demonstrate that MMP13 expression does not correlate with the number of activated HSCs and myofibroblasts, whereas TIMP-1 and collagen-1 decrease in proportion to the loss of activated HSCs from the liver (13, 19). Indeed, using in situ hybridization in serial sections of CCl_4-treated mouse liver, we detected abundant *timp1* transcript but only rare *mmp13* in scar-associated spindle cells. These data concur with previous studies which have identified HSCs as the primary source of inhibitory TIMPs in human liver disease (29) and in animal models of liver fibrosis both in vitro in cell culture models of HSC activation (30) and in vivo using in situ hybridization and immunohistochemistry (31). However, in our rodent models of liver fibrosis and spontaneous regression, HSCs are not a major source of MMP13.

The effect of MMP13 gene knockout has recently been studied in several animal models of tissue turnover and injury-repair in different organs. These studies have demonstrated that MMP13 plays an important role in bone development and remodeling and in collagen breakdown within atherosclerotic plaques (20, 32, 33), but not in epidermal wound healing (34). In a biliary fibrosis model of progressive liver injury, MMP13 deficiency attenuated hepatic inflammation and fibrosis (35). However, bile duct ligation is a complex model involving proliferation of stem cell components in association with myofibroblasts, whereas CCl_4 is a model of inflammation, repair and resolution. We have shown that MMP13 deficiency reduced the capacity of the liver to remodel scar by 5 days of recovery in a mouse model of advanced liver fibrosis, although gene deletion did not inhibit resolution completely. Chronic CCl_4 toxicity induced inflammatory and fibrotic liver injury that was similar in gene-deleted and WT mice such that our observations during the resolution phase were directly comparable. Interestingly, a perisinusoidal associated fibrosis persisted in $mmp13^{-/-}$ livers. This distribution of fibrillar collagen has been shown to be especially rich in SAMs after CCl_4 injury (1). The likely explanation for our $mmp13^{-/-}$ phenotype is partial compensation by other MMPs capable of degrading interstitial collagens (MMP8, MMP14, MMP2). Although for each individual MMP the trend toward up-regulation was not statistically significant in $mmp13^{-/-}$ mice relative to WTs (Table I), in combination these proteases might materially contribute to matrix degradation. Both MMP2 and MMP14 have been detected in animal models of liver fibrosis and in chronic hepatitis and cirrhosis in humans, with mRNA localizing to HSCs (36–38). They are also up-regulated during resolution of fibrosis, although the actions of MMP2 appear to be complex and somewhat paradoxical in that this enzyme may contribute to fibrogenesis via proproliferative effects on HSCs (32).

In contrast to humans, in whom MMP1 is expressed as the major interstitial collagenase, the ortholog of MMP1 (McolA) is expressed in mice at low levels (39). Instead, MMP13 is widely believed to remodel fibrillar collagen in rodent tissues. Despite structural and functional similarities, MMP1 and MMP13 show contrasting responses to cytokines and growth factors and have distinct MMP-dependent activation mechanisms (7). Therefore, one should not automatically assume that observations from rodent models of liver fibrosis are germane to human disease. Nevertheless, in preliminary studies using immunohistochemistry, we have demonstrated MMP13 protein expression in two separate cases of human alcoholic cirrhosis within large scar-associated phagocytes, consistent with our rodent studies (data not shown). As well as cleaving collagen-1 at a single locus in the triple helix, MMP13 cleaves collagen-1 at a site in the N telopeptide which destabilizes cross-linked collagen. This may facilitate the breakdown of mature, highly cross-linked collagen in tissues that have been rendered resistant to MMP1.

The identity and source of the rodent collagenase that mediates matrix remodeling in liver fibrosis has proved elusive, despite the importance of these data to the interpretation of models designed to determine the pathogenesis of fibrosis and provide proof of concept of potential therapies. The identification of SAMs as the primary source of interstitial collagenase (at least in rodents) represents a major advance in our understanding of fibrosis resolution. Our preliminary data in human cirrhosis indicate that MMP13 might also play a more prominent role in human liver fibrosis than was previously considered.

Acknowledgments

We thank Dr. Stephen Krane (Harvard Medical School, Boston, MA) for the gift of MMP13 knockout mice and Dr. Joseph Bonventre (Harvard Medical School) and Dr. Stuart Forbes (University of Edinburgh, Edinburgh, U.K.) for assistance.

Disclosures

J. P. Iredale is a consultant for GEC Healthcare advising on noninvasive diagnosis of fibrosis.

References

1. Duffield, J., S. Forbes, C. Constandinou, S. Clay, M. Partolina, S. Vuthoori, S. Wu, R. Lang, and J. Iredale. 2005. Selective depletion of macrophages reveals distinct, opposing roles during liver injury and repair. *J. Clin. Invest.* 115: 56–65.
2. Shapiro, S. D., D. K. Kobayashi, A. P. Pentland, and H. G. Welgus. 1993. Induction of macrophage metalloproteinases by extracellular matrix. *J. Biol. Chem.* 268: 8170–8175.
3. Shapiro, S. D., E. J. Campbell, D. K. Kobayashi, and H. G. Welgus. 1990. Immune modulation of metalloproteinase production in human macrophages:

Downloaded from http://www.jimmunol.org/ at North Dakota State Univ Lib/Periodicals Dept on June 5, 2015

selective pretranslational suppression of interstitial collagenase and stromelysin biosynthesis by interferon-γ. *J. Clin. Invest.* 86: 1204–1210.
4. McCachren, S. S. 1991. Expression of metalloproteinases and metalloproteinase inhibitor in human arthritic synovium. *Arthritis Rheum.* 135: 314–325.
5. Henney, A. M., P. R. Wakeley, M. J. Davies, K. Foster, R. Hembry, and G. Murphy. 1991. Localisation of stromelysin gene expression in atherosclerotic plaques by in situ hybridisation. *Proc. Natl. Acad. Sci. USA* 88: 8154–8158.
6. Perez-Ramos, J., M. Segura-Valdez, B. Vanda, M. Selman, and A. Pardo. 1999. Matrix metalloproteinases 2, 9, and 13, and tissue inhibitors of metalloproteinases 1 and 2 in experimental lung silicosis. *Am. J. Respir. Crit. Care Med.* 160: 1274–1282.
7. Knauper, V., C. Lopez-Otin, B. Smith, G. Knight, and G. Murphy. 1996. Biochemical characterization of human collagenase-3. *J. Biol. Chem.* 271: 1544–1550.
8. Wright, M. C., R. Issa, D. E. Smart, N. Trim, G. I. Murray, J. N. Primrose, M. J. P. Arthur, J. P. Iredale, and D. A. Mann. 2001. Gliotoxin stimulates the apoptosis of human and rat hepatic stellate cells and enhances the resolution of liver fibrosis in rats. *Gastroenterology* 121: 685–698.
9. Iimuro, Y., T. Nishio, T. Morimoto, T. Nitta, B. Stefanovic, S. K. Choi, D. A. Brenner, and Y. Yamaoka. 2003. Delivery of matrix metalloproteinase-1 attenuates established liver fibrosis in the rat. *Gastroenterology* 124: 445–458.
10. Thirunavukkarasu, C., Y. Yang, V. M. Subbotin, S. A. K. Harvey, J. Fung, and C. R. Gandhi. 2004. Endothelin receptor antagonist TAK-044 arrests and reverses the development of carbon tetrachloride induced cirrhosis in rats. *Gut* 53: 1010–1019.
11. Knauper, V., H. Will, C. Lopez-Otin, B. Smith, S. J. Atkinson, H. Stanton, R. M. Hembry, and G. Murphy. 1996. Cellular mechanisms for human procollagenase-3 (MMP-13) activation: evidence that MT1-MMP (MMP-14) and gelatinase A (MMP-2) are able to generate active enzyme. *J. Biol. Chem.* 271: 17124–17131.
12. Knauper, V., B. Smith, C. Lopez-Otin, and G. Murphy. 1997. Activation of pro-gelatinase B (pro-MMP-9) by active collagenase-3 (MMP-13). *Eur. J. Biochem.* 248: 369–373.
13. Iredale, J. P., R. C. Benyon, J. Pickering, M. McCullen, S. Northrop, S. Pawley, C. J. Hovell, and M. J. P. Arthur. 1998. Mechanisms of spontaneous resolution of rat liver fibrosis: hepatic stellate cell apoptosis and reduced hepatic expression of metalloproteinase inhibitors. *J. Clin. Invest.* 102: 538–549.
14. Benyon, R. C., J. P. Iredale, S. Goddard, P. J. Winwood, and M. J. P. Arthur. 1996. Expression of tissue inhibitor of metalloproteinases 1 and 2 is increased in fibrotic human liver. *Gastroenterology* 110: 821–831.
15. Watanabe, T., M. Niioka, S. Hozawa, K. Kameyama, T. Hayashi, M. Arai, A. Ishikawa, K. Maruyama, and I. Okazaki. 2000. Gene expression of interstitial collagenase in both progressive and recovery phase of rat liver fibrosis induced by carbon tetrachloride. *J. Hepatol.* 33: 224–235.
16. Hironaka, K., I. Sakaida, Y. Matsumara, S. Kaino, K. Miyamoto, and K. Okita. 2000. Enhanced interstitial collagenase (matrix metalloproteinase-13) production of Kupffer cells by gadolinium chloride prevents pig serum-induced rat liver fibrosis. *Biochem. Biophys. Res. Commun.* 267: 290–295.
17. Watanabe, T., M. Niioka, S. Hozawa, Y. Sugioka, M. Arai, K. Maruyama, H. Okano, and I. Okazaki. 2003. Stem cells expressing MMP-13 mRNA appear during regression reversal of hepatic cirrhosis. In *Extracellular Matrix and the Liver: Approach to Gene Therapy.* I. Okazaki, Y. Ninomiya, S. L. Friedman, and K. Tanikawa, eds. Academic Press, New York, pp. 361–388.
18. Knittel, T., M. Mehde, A. Grundmann, B. Saile, J.-G. Scharf, and G. Ramadori. 2000. Expression of matrix metalloproteinases and their inhibitors during hepatic tissue repair in the rat. *Histochem. Cell Biol.* 113: 443–453.
19. Issa, R., X. Zhou, C. M. Constandinou, J. Fallowfield, H. Millward-Sadler, M. D. Gaca, E. Sands, I. Suliman, N. Trim, A. Knorr, et al. 2004. Spontaneous recovery from micronodular cirrhosis: evidence for incomplete resolution associated with matrix cross-linking. *Gastroenterology* 126: 1795–1808.
20. Inada, M., Y. Wang, M. H. Byrne, M. U. Rahman, C. Miyaura, C. Lopez-Otin, and S. M. Krane. 2004. Critical roles for collagenase-3 (Mmp13) in development of growth plate cartilage and in endochondral ossification. *Proc. Natl. Acad. Sci. USA* 101: 17192–17197.
21. MacSween, R. N., V. J. Desmet, T. Roskams, and P. J. Scothorne. 2002. Developmental anatomy and normal structure. In *Pathology of the Liver.* 4th Ed. R. N. MacSween, A. D. Burt, B. C. Portmann, K. G. Ishak, P. J. Scheuer, and P. P. Anthony, eds. Churchill Livingstone, London, pp. 52–55.
22. Duffield, J. S., P. G. Tipping, T. Kipari, J. F. Cailhier, S. Clay, R. Lang, J. V. Bonventre, and J. Hughes. 2005. Conditional ablation of macrophages halts progression of crescentic glomerulonephritis. *Am. J. Pathol.* 167: 1207–1219.
23. Leibovich, S. J., and R. Ross. 1975. The role of the macrophage in wound repair: a study with hydrocortisone and antimacrophage serum. *Am. J. Pathol.* 78: 71–100.
24. Welgus, H. G., E. J. Campbell, J. D. Cury, A. Z. Eisen, R. M. Senior, S. M. Wilhelm, and G. I. Goldberg. 1990. Neutral metalloproteinases produced by human mononuclear phagocytes: enzyme profile, regulation and expression during cellular development. *J. Clin. Invest.* 86: 1496–1502.
25. Dayer, J. M., B. de Rochemonteix, B. Burrus, S. Demczuk, and C. A. Dinarello. 1986. Human recombinant interleukin-1 stimulates collagenase and prostaglandin E2 production by human synovial cells. *J. Clin. Invest.* 77: 645–648.
26. Danenberg, H. D., I. Fishbein, J. Gao, J. Monkkonen, and R. Reich. 2002. Macrophage depletion by clodronate-containing liposomes reduces neointimal formation after balloon injury in rats and rabbits. *Circulation* 106: 599–605.
27. Zhang-Hoover, J., A. Sutton, N. van Rooijen, and J. Stein-Streilein. 2000. A critical role for alveolar macrophages in elicitation of pulmonary immune fibrosis. *Immunology* 101: 501–511.
28. Popov, Y., E. Patsenker, M. Banner, E. Niedobitek, A. Schulze-Krebs, and D. Schuppan. 2006. Halofuginone induces matrix metalloproteinases in rat hepatic stellate cells via activation of p38 and NFκB. *J. Biol. Chem.* 281: 15090–15098.
29. Benyon, R. C., J. P. Iredale, S. Goddard, P. J. Winwood, and M. J. P. Arthur. 1996. Increased expression of tissue inhibitor of metalloproteinases-1 and -2 relative to interstitial collagenase in fibrotic human liver. *Gastroenterology* 110: 821–831.
30. Iredale, J. P., R. C. Benyon, M. J. P. Arthur, W. F. Ferris, R. Alcolado, P. J. Winwood, N. Clark, and G. Murphy. 1996. Tissue inhibitor of metalloproteinase-1 messenger RNA expression is enhanced relative to interstitial collagenase messenger mRNA in experimental liver injury and fibrosis. *Hepatology* 24: 176–184.
31. Nie, Q. H., G. R. Duan, X. D. Luo, Y. M. Xie, H. Luo, Y. X. Zhou, and B. R. Pan. 2004. Expression of TIMP-1 and TIMP-2 in rats with hepatic fibrosis. *World J. Gastroenterol.* 10: 86–90.
32. Stickens, D., D. J. Behonick, N. Ortega, B. Heyer, B. Hartenstein, Y. Yu, A. J. Fosang, M. Schorpp-Kistner, P. Angel, and Z. Werb. 2004. Altered endochondral bone development in matrix metalloproteinase 13-deficient mice. *Development* 131: 5883–5895.
33. Deguchi, J.-O., E. Aikawa, P. Libby, J. Vachon, M. Inada, S. Krane, P. Whittaker, and M. Aikawa. 2005. Matrix metalloproteinase-13/collagenase-3 deletion promotes collagen accumulation and organisation in mouse atherosclerotic plaques. *Circulation* 112: 2708–2715.
34. Hartenstein, B., B. T. Dittrich, D. Stickens, B. Heyer, T. H. Vu, S. Teurich, M. Schorpp-Kistner, Z. Werb, and P. Angel. 2006. Epidermal development and wound healing in matrix metalloproteinase 13-deficient mice. *J. Invest. Dermatol.* 126: 486–496.
35. Uchinami, H., E. Seki, D. A. Brenner, and J. D'Armiento. 2006. Loss of MMP13 attenuates murine hepatic injury and fibrosis during cholestasis. *Hepatology* 44: 420–429.
36. Takahara, T., K. Furui, J. Funaki, Y. Nakayama, H. Itoh, C. Miyabayashi, H. Sato, M. Seiki, A. Ooshima, and A. Watanabe. 1995. Increased expression of matrix metalloproteinase-II in experimental liver fibrosis in rats. *Hepatology* 21: 787–795.
37. Takahara, T., K. Furui, Y. Yata, B. Jin, L. P. Zhang, S. Nambu, H. Sato, M. Seiki, and A. Watanabe. 1997. Dual expression of matrix metalloproteinase-2 and membrane-type 1-matrix metalloproteinase in fibrotic human livers. *Hepatology* 26: 1521–1529.
38. Zhou, X., C. J. Hovell, S. Pawley, M. I. Hutchings, M. J. P. Arthur, J. P. Iredale, and R. C. Benyon. 2004. Expression of matrix metalloproteinase-2 and -14 persists during early resolution of experimental liver fibrosis and might contribute to fibrolysis. *Liver Int.* 24: 492–501.
39. Balbín, M., A. Fueyo, V. Knauper, J. M. Lopez, J. Alvarez, L. Sanchez, V. Quesada, J. Bordallo, G. Murphy, and C. Lopez-Otin. 2001. Identification and enzymatic characterization of two diverging murine counterparts of human interstitial collagenase (MMP-1) expressed at sites of embryo implantation. *J. Biol. Chem.* 276: 10253–10262.

Downloaded from http://www.jimmunol.org/ at North Dakota State Univ Lib/Periodicals Dept on June 5, 2015